

Cellular automata in damage mechanics: creep rupture case

M. CHRZANOWSKI, K. NOWAK

*Cracow University of Technology
Kraków, Poland*

IN THE PAPER, the cellular automata (CA) method for the description of damage formation introduced in [1], is extended over creep circumstance by introducing grain boundaries. The material structure is modelled by Voronoi-like tessellation with distance measure corresponding to Moore neighbourhood. The size of Representative Volume Element (RVE) is determined by the number of grains, seed nodes of which are distributed by a homogeneous Poisson point process. The global number of cells to be damaged is subjected to the mass conservation law. Additionally, probabilistic rules, which cause the damage to develop in form of microcracks, microvoids, large voids or a combination of voids and cracks are used. Loading through imposed deformation of RVE is continued until damage cells form a continuous path spanning opposite sides of RVE. In terms of continuum damage mechanics, this situation corresponds to the damage parameter reaching the critical value in a given material point. The results obtained in this paper for polycrystalline material have been compared with a material of homogenous structure.

1. Introduction

ENVIRONMENTAL EFFECTS (like external loading, high temperatures, periodical loading, chemical and magneto-electrical fields) superimposed upon engineering structures lead to their life-time exploitation (plastic limit state, creep and fatigue durability, corrosion, electrical breaks). These effects result from the irreversible processes which are caused by changes in the microstructure of a material. To bring them up on the macroscopic level, two strategies are common: to introduce a new state variable by the smoothing structural changes over a Representative Volume Element (RVE) (using the homogenization technique), or by describing direct relationship between microstructural changes and the searched effect, and relate them with state variables defined on macro-level. The former allows for effective solution to be obtained, but it falls into the frame of phenomenological description and therefore does not explain the physical reasons for observed phenomenon. For example, to describe creep rupture a damage parameter is introduced, along with its evolution law, which is incorporated into the system of state variable defined on macro-level and making use of the mathematical concept of convergence limit (stress, strain).

On the microscopic level, at which the concepts of *continuum mechanics* lose their meaning because of discrete nature of the matter, there is a strong need to relate structural changes to the phenomenon of practical interest (e.g. to relate void and slips formation in polycrystalline materials with material yielding or decohesion). In this case the state variable introduced by continuum mechanics can be dealt with as an external source of structural changes which occur on microscopic level. One has to admit that material constants which appear in evolution laws for macroscopic state variables are determined on the basis of macroscopic experiments. In such a way they confine all structural changes which occur on different dimensional levels (from meters to micrometers to nanometers) and therefore one should not feed back the evolution laws on a macroscopic level.

The present paper falls into the frame of the latter approach. The stress and/or strains calculated on macroscopic level are applied to a RVE with internal structure and its changes are modelled by means of a cellular automaton (CA). The motivation for the use of CA is given in a separate section.

The main goal of the paper is to model the creep failure of polycrystalline materials (metals and their alloys), following and modifying the proposition offered by MATIC and GELTMACHER in [1].

2. Creep rupture – physics and phenomenology

The process of material fracture in creep conditions is activated by high temperature. This is a complex process and different mechanisms are distinguished for polycrystalline materials (cf. e.g. [2]). As an example, in Fig. 1 the failure

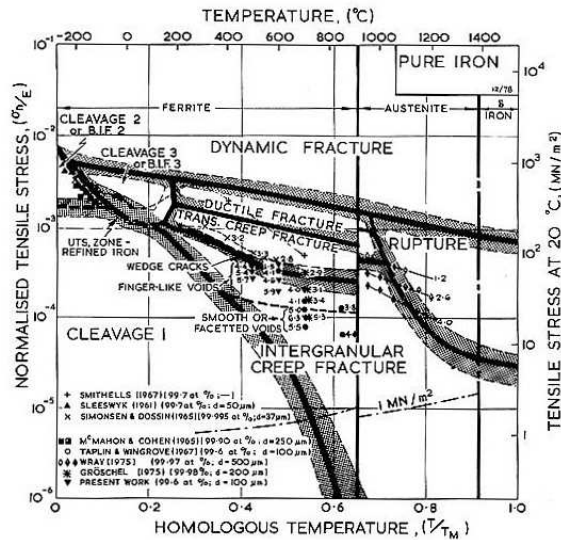


FIG. 1. Fracture mechanism map for pure iron [3].

map for pure iron is shown, based on identification of metallurgical phenomena. In engineering applications, the creep deformations (not shown in this figure) come to play an important role in temperature range of 0.4 – 0.7 of the homologous scale. It is seen that in this range there are numerous mechanisms which may lead to creep rupture: wedge cracks, finger-like voids, smooth or faceted voids. Two extreme cases: ductile failure which occurs at relatively high stresses and the brittle one (designated with the name of intergranular fracture in Fig. 1) are of prime importance. The former one (called also transgranular failure) is mostly caused by slip bands formed across grains, whereas brittle failure is associated with mechanisms occurring on grain boundaries (triple point cracks, voids etc.). In the intermediate region of stress level all these mechanisms develop and interact leading to the so-called mixed-mode failure. It follows that if any description related to the material structure is concerned, then the distinction between grains and their boundaries has to be made.

The effects of the above sketched micro-processes can be traced also in macro-scale. For different stress levels the time to failure and stress-strain diagrams, shown schematically in Fig. 2, exhibit physical micro-processes which are hidden behind them. On the diagram of stress and time to failure t_R (for uniaxial tension), one can identify the same three types of failure described above: ductile, mixed-mode and brittle ones. In turn, the same stress levels produce different creep curves (Fig. 2b). For low stress, the time to failure is large but the deformation at this time is rather small. For high stresses, the shape of deformation curves changes drastically (e.g. no steady-state creep is observed) and the deformation at relatively short time to failure is large.

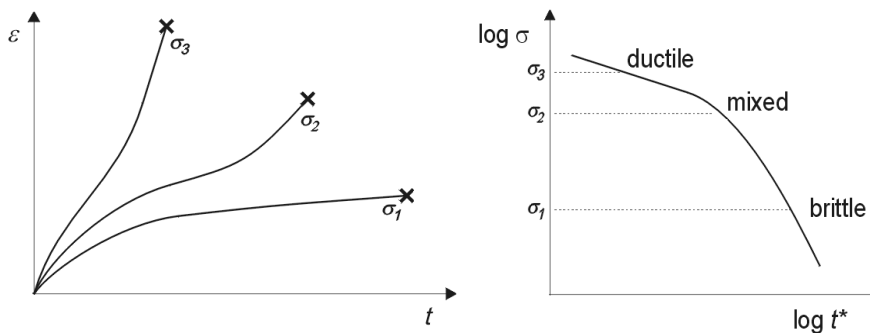


FIG. 2. Schematic relation between creep curves and creep failure modes.

In continuum mechanics, phenomenological description of the above processes is attained by introduction of suitable state variables. Besides standard variables of stress and strain, which are defined through mathematical limit concept and are based on the assumption of material continuity, the new state variables are introduced. If these new variables aim at the description of discrete phenomena

(like micro-cracking of internal material structure), the technique of homogenization is used to bring them to the macroscopic level. Such an approach yielded the formation of a new branch of failure mechanics – continuum damage mechanics (named in [4] CDM). The evolution law for a scalar damage variable (which in general should be of tensorial character) is often assumed to be a function of stress state (cf. [5]):

$$(2.1) \quad \frac{\partial \psi}{\partial t} = A \left(\frac{\sigma}{\psi} \right)^m,$$

where ψ is a continuity parameter ($1 \geq \psi \geq 0$).

A full description of the deformation and failure process requires coupling of the above equation with the stress-strain rate relationship. The analysis of the number of practical problems (cf. e.g. [6]) was performed using the set of equations:

$$(2.2) \quad \begin{aligned} \frac{\partial \varepsilon_{ij}}{\partial t} &= D_{ijkl}^{-1} \frac{\partial \sigma_{ij}}{\partial t} + \gamma \left(\frac{\sigma_{\text{eff}}}{1 - \omega} \right)^n \frac{\partial \sigma_{\text{eff}}}{\partial \sigma_{ij}}, \\ \frac{\partial \omega}{\partial t} &= A \left[\alpha \frac{\sigma_{\text{max}}}{1 - \omega} + (1 - \alpha) \frac{\sigma_{\text{eff}}}{1 - \omega} \right]^m, \end{aligned}$$

where D_{ijkl} is the elastic constants matrix, γ , n are steady-state creep constants, A , m , α are damage material constants; σ_{eff} is the Huber–Mises effective stress, σ_{max} is the main positive principal stress, t is time, ε_{ij} and σ_{ij} are strain and stress tensors, $\omega = 1 - \psi$ is the scalar damage parameter ($0 \leq \omega \leq 1$).

The phenomenological description on the macro-level of *material continuum* does not account directly for processes which occur on micro-level. To attain this effect one has to introduce the methods of discrete analysis of phenomena on the level at which these phenomena occur.

3. Motivation for the use of CA

The structure of a material on microscopic level is obviously of a discrete character. This precludes the use of state variables which have been defined for a *continuum*. The most appropriate solution is to use discrete description for a discrete phenomenon. Such a possibility is offered by CA which by their nature are of discrete character.

The concept of CA was pursued by von Neumann in the 40-ties of the last century, following the theoretical consideration of self-reproductive systems by a Polish mathematician Stanislaw Ulam.

A cellular automaton is defined solely by definition of (cf. [7]):

- a cell network in space of D dimension,

- a set of cell states,
- an evolution rule of the cell state.

The last of the above rules confines both: the state of the cell and the states of its neighbours. Therefore this neighbourhood has to be defined, too.

The CA have been used in metal forming description (cf. e.g. [8, 9]). Recently, it has been applied also to the description of damage formation in metals subjected to plastic deformation. In the paper by MATIC and GELTMACHER [1] the influence of the neighbouring cells upon the state of a cell is searched thoroughly. The analysis is confined to the RVE behaviour under biaxial plane strain of the magnitude up to 20%. The influence of the neighbours is taken into account by four different rules, however there is no distinction between grain and grain boundaries.

In the present paper an attempt to use the same methodology for creep failure is made. To distinguish between the described above modes of failure: brittle and ductile one, modelling of grains and grain boundaries is necessary.

4. Modelling of material structure

The description of phenomena, which take place on microstructural level, requires a choice of RVE of proper size. As in this paper an attempt is made to describe the phenomena which occur along grain boundaries or throughout individual grains, then RVE has to contain more than one grain up to several hundreds of grains. One of the paper goals will be to search out how the size of RVE influences the results. It is obvious that this size has to be below the macroscopic dimension of the structure. For example, for grains size of the order of 100 μm (typical for metals and their alloys), the linear characteristic size of RVE should be of the order of 1 mm.

The behaviour of the material structure within RVE will be determined by two-dimensional CA with Moore neighbourhood. Each cell of the automaton is defined by a single state variable g which can take the values $g = -1, 0, 1, \dots, G$, where -1 denotes a cell outside RVE, 0 – an *empty* cell with destructed material within RVE, and $1, \dots, G$ are grain numbers within RVE. For all values of $g > 0$ the cell corresponds to non-destructed material (*mass cell*). Different values of $g > 0$ in neighbouring cells defines the grain boundary and in such a way, the rule of automaton can take into account existence of grain boundaries.

The same automaton, but with a different evolution rule, is used for modelling the initial structure of a material. The concept of the Voronoi tessellation is used with distance measure between seed points according to the definition of the Moore neighbourhood [10]. This results in diversified shapes of individual grain, including convex and concave grains as well. The seed points are distributed by

a homogeneous Poisson point process. Number of seed points corresponds to the number of grains in RVE. No distinction is made with respect to the physical properties of different grains or to their crystallographic orientation.

The rule for this automaton is as follows:

$$(4.1) \quad F_{i+1}(x) = \begin{cases} F_i(x) & \text{if } F_i(x) \neq 0 \\ \text{Mean}(F_i(y) : y \in \text{Neighbourhood}(x) \text{ and } F_i(y) > 0) & \text{if } F_i(x) = 0 \end{cases}$$

where x is a cell, F_i denotes a function of state in step i , *Mean* is a function returning mean value rounded to the closest integer, *Neighbourhood*(x) is a function returning the set of all neighbours of x . The rule is executed until all cells of RVE are filled with mass cells.

An example of initial material structure is shown in Fig. 3 for the number of seed points equal to 100.

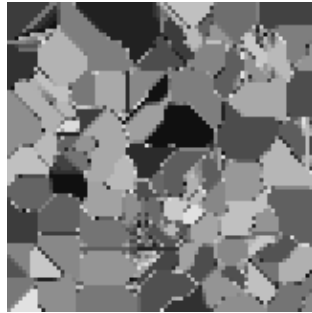


FIG. 3. An example of initial material structure.

5. Damage evolution by means of CA

The loading of RVE is done by imposing homogeneous, symmetric biaxial plane-strain deformation. The number of automaton cells corresponding to the initial stage of the RVE N_0 defines the consecutive time steps of the RVE growth. The initial number of cells should be such that the next stretching will correspond to the strain which is a small fraction of deformation at failure. In this paper, the influence of initial cell numbers upon the strain to failure is searched out starting from 81×81 . If one assumes that RVE is stretched by 2 cells for each stage (to maintain symmetry) then the first logarithmic strain will be $\log(1 + 2/81) = 2.4\%$, and the consecutive deformation steps will be smaller.

The damage growth is determined by the mass conservation law and by probabilistic automaton rules (state of given cells and their neighbours). From the

mass conservation law follows the total number of automaton cells the state of which has to be defined as *empty*. This is equal to the total number of automaton cells corresponding to the actual RVE size, minus the number of mass cells in initial state $N_0 \times N_0$. Cells to be emptied are found out in two steps. The parameter β ($0 \leq \beta \leq 1$) defines the portion of a cell to be emptied in the first of these steps, in which the projection of mass distribution over CA covering the deformed state of RVE is the only criterion. The value of *fractional mass* is calculated for each cell x corresponding to a given grain $m_{i+1}^*(x, g)$. For the cell which belongs to two or more grains, the maximum fractional mass defines the grain to which the given cell belongs – $g_{\max}(x)$. So the fractional mass for a cell is:

$$(5.1) \quad m_{i+1}(x) = m_{i+1}^*(x, g_{\max}(x)).$$

This fractional mass is compared with threshold value, and any cells with mass below this value are set to be empty (their state is equal to 0). The threshold value is calculated in each stage in such a way that the number of cells that remain mass cells conform to the number the cells to be emptied.

In the second step, the damage in remaining cells to be emptied is evaluated according to the rules of the automaton. Mean probability p_0 of the mass cell to be emptied in the second step is defined by the number of a cells to be emptied in this step. Depending on the cell neighbourhood, the probability of a cell to be emptied $p(z)$ is calculated through weighing functions $w(z)$ associated with the automaton rules:

$$(5.2) \quad \begin{aligned} p(z) &= p_0 \cdot w(z), \\ w(z) &= \frac{b(z) \cdot \sum n(z)}{\sum (b(z) \cdot n(z))}, \end{aligned}$$

where z is the type of neighbourhood; in the case of Moore, the total number of neighbourhoods is equal to 256. Function $n(z)$ yields the number of cells with a given type of neighbourhood z . Multiplier $b(z)$ for weighing function $w(z)$ can be an arbitrary, nonnegative number, and is to be chosen depending on the prevailing mechanism of damage formation. The summation in Eq. (5.2) extends over all types of neighbourhoods z . By setting the values of b , for all types of neighbourhood one can define a particular rule.

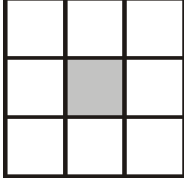
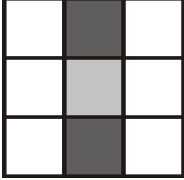
Following the classification given in [1], four probabilistic rules are introduced to distinguish different mechanisms:

- rule 0 – microcracks,
- rule 1 – microvoids,
- rule 2 – large voids,
- rule 3 – combined.

Names of the above rules are associated with the prevailing mechanism of damage formation.

An example of multiplier values $b(z)$ chosen for some neighbourhood types is shown in the table below. For complete definition of value b for all neighbourhood types, please refer to [1].

Table 1. Example of multiplier for weighing function. White cells are *mass*, black are *empty*, and grey are *mass* cells for which the probability is calculated.

rules:	Examples of neighbourhood types:		
			
	multipliers b for weighing function:		
0	1	100	1
1	1	1	1
2	1	0.01	100
3	1	100	10 000

Whole procedure is repeated over the consecutive steps. It is terminated when the empty cells produce an uninterrupted path spanning opposite sides of RVE; the corresponding strain is denoted as ε^f . Figure 4 shows final states of

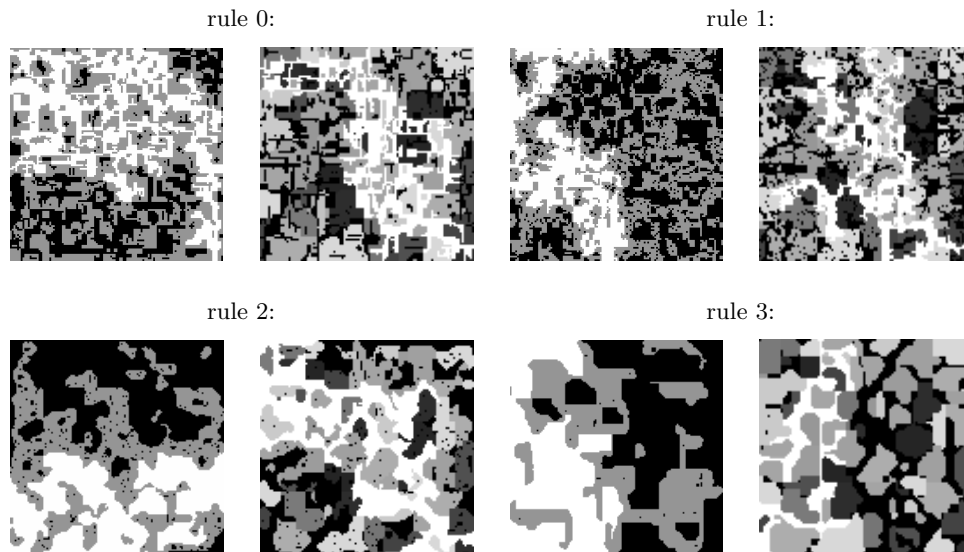


FIG. 4. The comparison of final damage states in RVE. On the left side – no grain boundaries; on right – with grains. Empty cells forming path spanning opposite sides are white, the remaining empty cells are black.

the fractured RVE for different rules, compared with analogous simulation when the grain boundaries are not taken into account.

6. Conclusions

The analysis of results is focused on the failure deformation. Parameters of the analysis are:

- the number of seed points G which is equivalent to the size of RVE if the mean grain size is fixed, or to the grain size if RVE is set,
- damage evolution rules of the automaton, and
- initial size of active automaton N_0 .

The results are referred to the case when no grain boundaries are taken into account ($G = 1$). In all cases the value of parameter β was set to 0.25. Figure 5 shows the influence of number of grains in RVE upon the failure strain depending on the rules 0, 1, 2, and 3 for different initial size of RVE with active automaton $N_0 = 81, 161,$ and 321 .

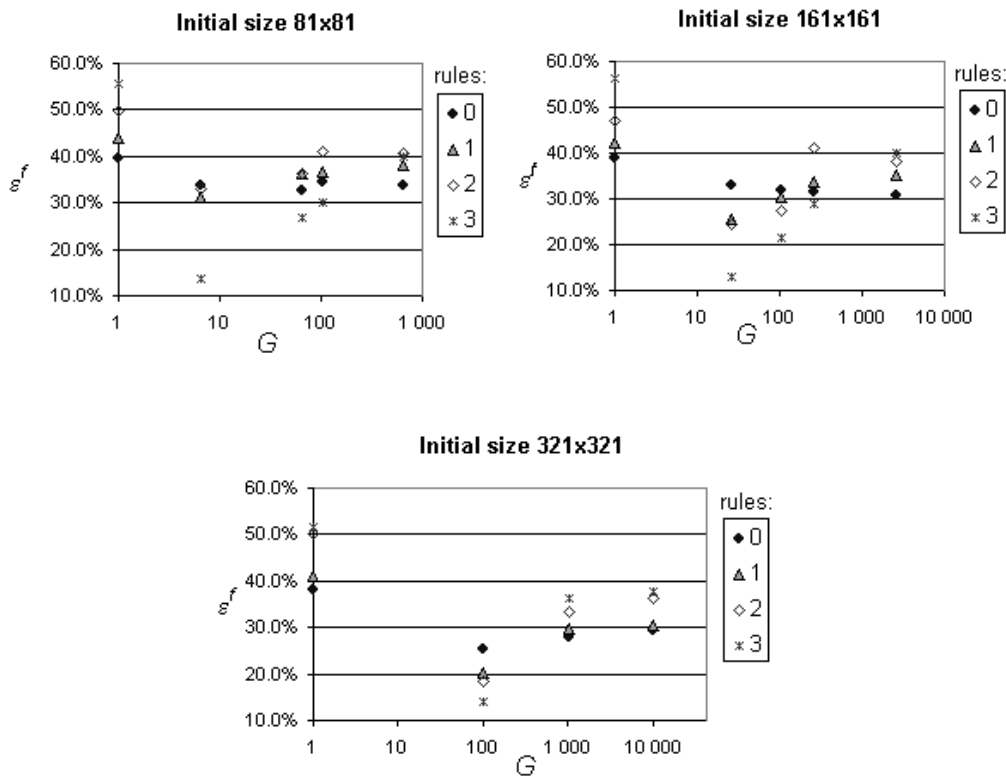


FIG. 5. Influence of problem parameters upon the mean value of failure strain.

It is easily seen that introduction of grain boundaries into the process description reduces the failure strain. The lower is the number of grains in an RVE, the higher is the reduction. Some regularity can be observed also with respect to the failure mechanisms. For mechanisms described by rules 0 (microcracks) and 1 (microvoids), the influence of grain numbers is the lowest. The decisive role plays the mechanism of large void creation (rule 2), which can be connected with triple point cracks formation at grain boundaries. Combining of this mechanism with microcracks (rule 3) fortifies this effect.

As the description proposed here is of nondeterministic character (both the structure modelling and damage formation are controlled by probabilistic rules), then the scatter of results is of importance. It is illustrated by Fig. 6 for the number of grains set to $G = 103$ and compared with the model without grains $G = 1$.

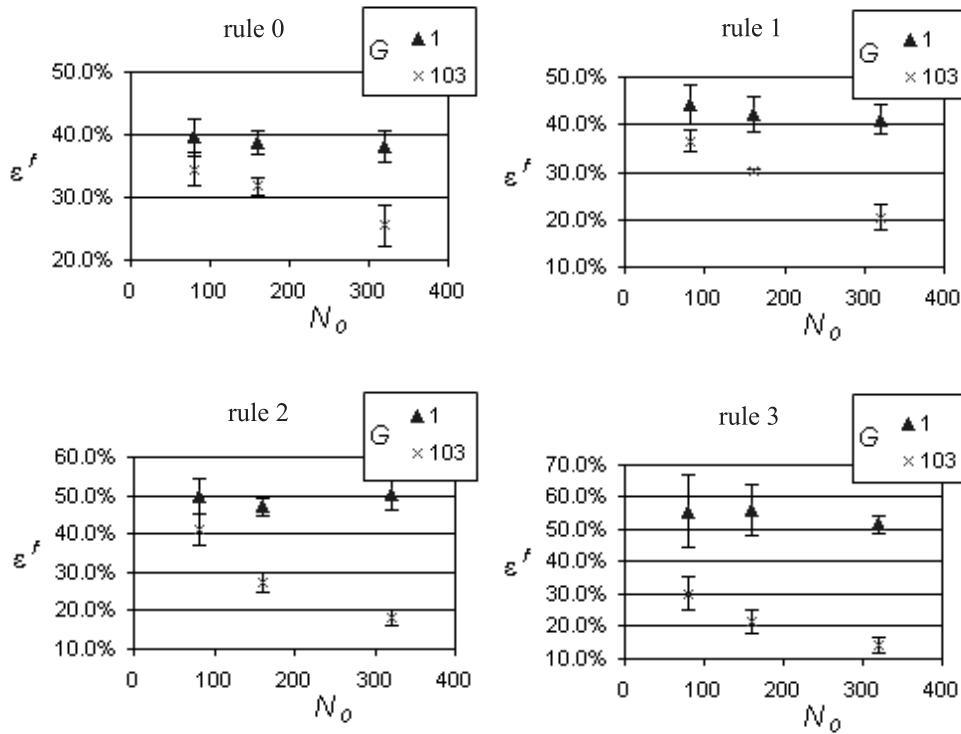


FIG. 6. Mean value and standard deviation of failure strain as a function of automaton resolution.

The mean value of failure strain is decreasing with initial size of active automaton N_0 , which can be called automaton resolution, for the proposed model with grain boundaries taken into account. If grain boundaries are not considered,

then the mean value of failure strain remains practically constant. Therefore, to obtain the results closer to that encountered in creep situation (failure strain of the order of several percent), the grain boundaries must be taken into account. The standard deviation is larger for a no boundaries model. It decreases for both models (with and without grains) when automation of higher resolution is used. This suggests that the automaton sensitivity has to correspond with the scale of considered processes.

The grain boundaries when taken into account reduce the value of failure deformation in all cases. The highest reduction is associated with the rule 3. But still the failure deformation is higher than that observed experimentally.

References

1. P. MATIC, A. B. GELTMACHER, *A cellular automaton-based technique for modeling multiscale damage evolution*, Computational Materials Science, **20**, 120–141, 2001.
2. R. J. FIELDS, T. WEERASOORIYA, M. F. ASHBY, *Fracture Mechanisms in Pure Iron, Two Austenitic Steels and One Ferritic Steel*, Metall. Trans. A., **11A**, 2, 333–347, 1980
3. NIST, Annual Report, Metallurgy Division of MSEL, National Institute of Standards and Technology, http://www.metallurgy.nist.gov/mechanical_properties, 2001.
4. J. JANSON, J. HULT, *Fracture mechanics and damage mechanics – a combined approach*, J. de Méc. Appliquée, **1**, 69–84, 1977.
5. L. M. KACHANOV, *On creep rupture time* [in Russian], Izv. AN SSSR OTN, **8**, 26–31, 1958.
6. A. BODNAR, M. CHRZANOWSKI, *On creep rupture of rectangular plates*, ZAMM, **82**, 201–205, 2002.
7. K. KUŁAKOWSKI, *Cellular Automata* [in Polish], OEN AGH, Kraków 2000.
8. S. DAS, E. J. PALMIERE, I. C. HOWARD, *Modelling Recrystallisation During Thermomechanical Processing Using CAFE*, Materials Science Forum, **467–470**, 1, 623–628, 2004.
9. J. GAWĄD, P. MACIOŁ, M. PIETRZYK, *Multiscale Modelling of Microstructure and Macroscopic Properties in Thixoforming Process Using Cellular Automation Technique*, Archives of Metallurgy and Materials, **50**, 549–562, 2005.
10. A. I. ADAMATZKY, *Voronoi-Like Partition of Lattice in Cellular Automata*, Mathematical and Computer Modelling, **23**, 4, 51–66, 1996.

Received December 11 2006; revised version April 2, 2007.
